Carbohydrate Research 346 (2011) 442–448

Contents lists available at ScienceDirect

Carbohydrate Research

journal homepage: www.elsevier.com/locate/carres

A combined theoretical and spectroscopic study of 4,6-di-*O*-acetyl-2,3-dideoxy-D-*erythro*-hex-2-enopyranosyl sulfamide: a novel glycosyl carbonic anhydrase IX inhibitor

Martín J. Lavecchia [a], Reinaldo Pis Diez [a,*], Pedro A. Colinas [b,*]

[a] CEQUINOR, Centro de Química Inorgánica (CONICET, UNLP), Departamento de Química, Facultad de Ciencias Exactas, Universidad, Nacional de La Plata CC 962, 1900 La Plata, Argentina
[b] LADECOR, Departamento de Química, Facultad de Ciencias Exactas, Universidad Nacional de La Plata, 47 y 115, 1900 La Plata, Argentina

ARTICLE INFO

Article history:
Received 26 March 2010
Received in revised form 8 July 2010
Accepted 13 July 2010
Available online 13 January 2011

Keywords:
Sulfamides
Carbonic anhidrase inhibitor
Density functional theory

ABSTRACT

The novel 4,6-di-*O*-acetyl-2,3-dideoxy-D-*erythro*-hex-2-enopyranosyl sulfamide, which exhibits selectivity for inhibiting isoform IX of carbonic anhydrase as overexpressed in many tumors, has been investigated from a combined theoretical and spectroscopic point of view. The conformational study of the compound shows that the α-anomeric form is more stable than the β-anomeric form from a thermodynamic point of view after including solvent effects. This fact suggests that the synthesis reaction could take place mainly under thermodynamic control as the main experimental product is the α-anomeric form of the sulfamide. Calculated α/β ratio is about 95:5, in excellent agreement with experimental data. Optimized geometries of the α-anomeric form agree quite well with crystallographic data. The inclusion of a solvent has negligible effects on the conformations. A detailed analysis of some geometric parameters shed light into the conformational behavior of the sulfamide in terms of both *exo*- and *endo*-anomeric effects and antiperiplanar relationships. Natural bond orbital calculations confirm those findings. Several intramolecular hydrogen bonds, characterized through the Atoms-in-Molecules theory, were found in the stable conformers. They, however, seem to play no relevant role in determining the relative stability of α conformers with respect to the β ones. Calculated ^{1}H and ^{13}C NMR chemical shifts support previous findings concerning configuration and conformation assignments of the title sulfamide. The IR spectrum of the compound is recorded and reported for the first time and the assignment of some of the most important bands is accomplished with the aid of calculated harmonic vibrational frequencies.

1. Introduction

Carbonic anhydrase (CA) is a metalloenzyme that catalyze the hydration of CO_2 and the dehydration of bicarbonate.[1] Up to now, 16 isozymes of CA have been described, with different subcellular localization and catalytic activity.[2] Recently, it has been shown that two CA isozymes (CA IX and to a less extent CAXII) are overexpressed in many tumors and absent in most normal tissues.[3] CA IX is responsible for the hypoxia-induced acidification of the extracellular environment of hypoxic tumor cells. Acidification increases the invasive behavior of cancer cells. Therefore, CA IX expression was associated with tumor propagation, malignant progression, and resistance to chemotherapy and radiotherapy. Thus, the inhibition of this isozyme is the target for the development of novel antitumor therapies. To minimize side effects, the inhibitor should exhibit selectivity for inhibiting the tumor-associated isoforms CA IX and XII over the ubiquitous isozyme CA II.

A new approach has been developed during the last few years for the design of effective CA inhibitors. The sugar approach consists of attaching a carbohydrate moiety to the metal-binding function that interacts with the active site, the zinc ion in this case.[4] The role of the carbohydrate moiety is, however, to facilitate selective or preferential inhibition of transmembrane CAs over cytosolic CAs. The stereochemical and structural variability of the glycosyl scaffold also provide the opportunity for interrogation of subtle differences of active site architecture among different CA isozymes. Our approach has been to tether a carbohydrate moiety to the high-affinity sulfamide CA pharmacophore, leading to *N*-glycosyl sulfamides.[5]

Recently, one of our groups reported the synthesis of novel *N*-glycosyl sulfamides by the addition of sulfamide to acetyl-protected D-glycals via Ferrier rearrangement on treatment with $BF_3{\cdot}OEt_2$.[6] These compounds were evaluated as inhibitors of four physiological CA isoforms, the ubiquitous hCA I and II as well the transmembrane, tumor associated hCA IX and hCA XII.[7] One of these compounds, the α anomer of 4,6-di-*O*-acetyl-2,3-dideoxy-

* Corresponding authors.
E-mail addresses: pis_diez@quimica.unlp.edu.ar (R.P. Diez), pcolinas@quimica.unlp.edu.ar (P.A. Colinas).

0008-6215/$ - see front matter © 2010 Elsevier Ltd. All rights reserved.
doi:10.1016/j.carres.2010.07.019

D-*erythro*-hex-2-enopyranosyl sulfamide, α-SAE for short, exhibited selectivity for inhibiting isoform hCA IX. α-SAE was found to be ten times less effective CA II inhibitor than its *threo* epimer, 4,6-di-*O*-acetyl-2,3-dideoxy-α-D-*threo*-hex-2-enopyranosyl sulfamide. A clash between 4-*O*-acetyl moiety of SAE and an amino acid residue, within the hCA II active site, was proposed as an explanation of its decreased affinity. This interaction is not present in its *threo* epimer, which shows a good binding to the enzyme.

SAE also shows micromolar antiproliferative activity in vitro against human lung and hepatocellular carcinoma cell lines.

Very recently, the conformational behavior of SAE was investigated by single X-ray diffraction and high-resolution NMR spectroscopy.[8] The $^{O}H_5$ was found to be the preferred conformation for this glycosyl sulfamide both in the crystal lattice and in solution. Moreover, a sulfonamide related to SAE was recently studied from a theoretical point of view, shedding light into its conformational behavior and its magnetic and vibrational properties.[9] As a continuation of our joint studies on *N*-glycosyl sulfamides, the conformational behavior of SAE, as well as its vibrational and magnetic properties is investigated from a computational viewpoint and is also compared with the experimental results. The goal of the present work is to contribute to the understanding and development of rational drug design of glycosyl sulfamides.

2. Methodology

2.1. Computational method

The conformational space of SAE is firstly investigated using molecular dynamics simulations.

As anomers of the 2,3-enopyranosyl systems could be present in two equilibrium conformations, namely $^{O}H_5$ and $^{5}H_O$, four different starting conformations of SAE are considered. The reference plane of the carbohydrate half-chair is defined by the four adjacent coplanar atoms, C1, C2, C3, and C4, with the ring oxygen atom, O1, and the C5 atom lying above or below this plane,[10] see Figure 1 for atom labels.

Moreover, each of these conformations is constructed both in α and β anomeric forms, according to the orientation of the sulfamide group. Starting conformations are labeled 1–4, see Figure 2 for labeling convention.

The conformational space of the four species mentioned above is investigated using molecular dynamics simulations as implemented in the HyperChem package.[11] The semiempirical AM1 method[12] was used as the force field.

Two simulations are performed for each conformer, differing only in the final temperature. The molecules are heated from 0 to 500 K in 0.1 ps in one case and from 0 to 700 K in 0.1 ps in the other case. The system temperature is then kept constant by coupling the system to a thermal bath with a bath relaxation time of 0.5 ps.[13] After an equilibration period of 10 ps, a 500 ps-long simulation is carried out storing the molecular cartesian coordinates every 10 ps. The time step for all the simulations is 1.0 fs.

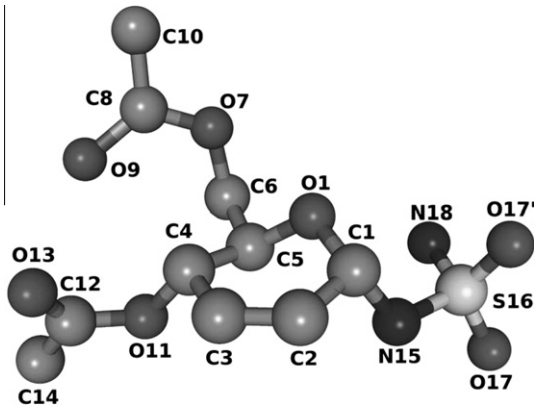

Figure 1. Numbering scheme of 4,6-di-*O*-acetyl-2,3-dideoxy-D-*threo*-hex-2-enopyranosyl sulfamide used throughout the work. Hydrogen atoms are not shown.

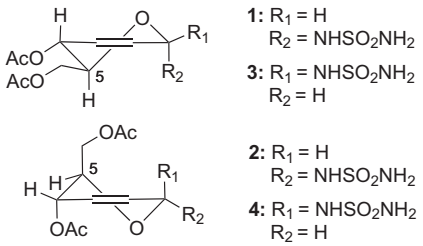

Figure 2. Schematic representation of the four starting conformations of 4,6-di-*O*-acetyl-2,3-dideoxy-D-*threo*-hex-2-enopyranosyl sulfamide. **1** and **2** correspond to the α anomeric form and **3** and **4** represent the β one.

Those geometries stored during the simulations are then optimized using the semiempirical AM1 method as implemented in the HyperChem package. Only those optimized geometries lying up to 2 kcal mol^{-1} above the lowest-energy conformer of every molecule are considered for further studies. The energy threshold of 2 kcal mol^{-1} provides some confidence that the contribution of higher energy conformations is less than 2% to every property measured at 298.15 K, according to the Maxwell–Boltzmann distribution.

The AM1-optimized geometries are further optimized using tools from the density functional theory[14–16] as implemented in the GAUSSIAN 03 package.[17] The optimizations are accomplished using the Becke's three parameters hybrid density functional[18] with the gradient-corrected correlation functional due to Lee, Yang, and Parr,[19] a combination that gives rise to the well-known B3LYP method.[20] The 6-31++G(d,p) basis set is used for all atoms.

The Hessian matrix is calculated at the B3LYP/6-31++G(d,p) level of theory and it is diagonalized for all the optimized geometries to verify whether they are local minima or saddle points on the potential energy surface of the molecules. The eigenvalues of the Hessian matrix are converted to vibrational frequencies, which are used to help in the assignment of the experimental IR spectrum. The calculated frequencies are scaled by a factor of 0.964,[21] which corresponds indeed to the B3LYP/6-31+G** level of theory as no scaling factor is reported for the method used in the present work. These calculations are also carried out with the GAUSSIAN 03 package.

^{1}H and ^{13}C isotropic shielding tensors are calculated at the B3LYP/6-311+G(2d,p)[22] level of theory using the Gauge-Including Atomic Orbital method,[23,24] as implemented in the GAUSSIAN 03 package. The isotropic shieldings are turned into chemical shifts by subtracting the corresponding isotropic shieldings of tetramethylsilane (TMS), which are calculated at the same level of theory.

To get an insight into the influence of the different anomeric effects over the relative stabilities of the conformers, a natural bond orbital (NBO)[25] analysis is carried out at the B3LYP/6-31++G(d,p) level of theory. The GAUSSIAN 03 package is used to this end.

The possibility of intramolecular hydrogen bonds in SAE, as a potential fact in determining relative stabilities, is analyzed within the framework of the Atoms-in-Molecules (AIM) theory.[26] Electronic densities obtained at the B3LYP/6-31++G(d,p) level of theory and the AIMAll package[27] are used for the AIM study.

A better comparison between experimental data and calculated properties could be obtained by including those conformers lying above the lowest-energy conformers up to 2 kcal mol^{-1} in a Maxwell–Boltzmann statistical-average at 298.15 K according to:

$$\langle \delta \rangle = \frac{\sum_j \delta_j e^{-\frac{E_j}{RT}}}{\sum_j e^{-\frac{E_j}{RT}}}$$

where δ_j is the corresponding property, conformer contribution, vibrational frequencies, and chemical shifts in the present work, of the jth conformer and E_j is its relative energy.

To analyze the effect of acetonitrile on the conformational behavior of SAE, solvent effects are taken into account in the present calculations through the conductor-like solvation model, as developed in the framework of the Polarizable Continuum Model (C-PCM).[28,29] Gas-phase geometries are re-optimized within the C-PCM model. Hessian matrices are constructed and diagonalized to confirm whether those structures are local minima or saddle points. Finally, the NBO and AIM analyses are performed on the freshly optimized geometries.

2.2. Experimental

FTIR spectrum of SAE is recorded with a Bruker Equinox 55 FTIR instrument, using the KBr pellet technique. The spectrum was registered in the 4000–400 cm^{-1} range at a temperature of 25 °C.

3. Results and discussion

The methodology described above leads to five different conformations in the gas phase, four of them belonging to the α anomeric form, conformation **1**, and the remaining representing the β anomer, conformation **3**. Conformations **2** and **4** are found to be higher in energy than the threshold of 2 kcal mol^{-1} and, thus, they are not considered for further analysis.

Table 1 lists some selected dihedral angles, for both the gas-phase and the solvent geometries, the differences in Gibbs free energy relative to the most stable conformation in every phase, and the relative contribution of every conformation at 298.15 K according to the Maxwell–Boltzmann statistical average. It is very interesting to note that the inclusion of solvent effects has little impact on the former, gas-phase geometries. However, the effect of solvation on the total electronic energies and the thermal corrections that lead to the Gibbs free energy is appreciable. Gas-phase results show that the relative composition at 298.15 K is about 61% in the β anomeric form of SAE and about 39% in the α form, according to the present calculations. When solvent effects are taken into account, the relative composition at 298.15 K is reversed to about 5% in the β anomeric form of SAE and about 95% in the α form, in excellent agreement with experimental results.[6] It should also be noted that the five stable conformers reported in this work exhibited the $^{O}H_5$ conformation with C1–O1–C5–C4 dihedral angles around the ideal value of 64°[30] and the acetoxymethyl group at C5 in a pseudo-equatorial position. It can also be seen from the table that other angles such as τ(N15–C1–C2–C3), τ(N15–C1–O1–C5), τ(C2–C1–N15–S16), and τ(O1–C1–N15–S16) indicate that the solid structure adopts the α anomeric form. Interestingly, the τ(C4–C5–C6–O7) and τ(O1–C5–C6–O7) dihedral angles seem to favor the **1a** conformer over the other α conformers.

It is also of interest to compare some selected bond lengths and bond angles involving the O1–C1–N15 acetal moiety in the different conformers with experimental data. The calculated O1–C1–N15 bond angle in the four pseudo axially substituted conformers **1** agrees very well with the crystal structure results (**1a**: 113.4° (112.8°); **1b**: 114.2° (113.7°); **1c**: 114.2° (113.8°); and **1d**:114.0° (113.5°); experimental: 112.7°,[8] calculated values in acetonitrile are in parenthesis). On the other hand, the O1–C1–N15 bond angle calculated for the pseudo equatorially substituted conformer **3a** (109.2° (108.7°)) is considerably lower than the experimental value. These facts are in good agreement with previous studies of bond angle variations in acetals.[31] The C1–N15 bond length in conformer **3a** (1.444 Å (1.450 Å)) is shorter than the values in conformers **1** (**1a**: 1.456 Å (1.466 Å); **1b**: 1.459 Å (1.464 Å); **1c**: 1.454 Å (1.465 Å); **1d**: 1.460 Å (1.463 Å)) and in the solid-state conformation of the α anomer (1.463 Å). These findings could be explained in terms of a competition between a $n_{N15} \rightarrow \sigma^*_{C1-O1}$ orbital interaction (*exo*-anomeric effect) and a $n_{O1} \rightarrow \sigma^*_{C1-N15}$ orbital interaction (*endo*-anomeric effect) in α conformers. In the conformer **3a** the

Table 1
Selected torsion angles, in degrees, of the five stable conformers of 4,6-di-*O*-acetyl-2,3-dideoxy-D-*threo*-hex-2-enopyranosyl sulfamide found within 2 kcal mol^{-1} with respect to the most stable one in the gas phase

	3a	**1a**	**1b**	**1c**	**1d**	Exp.[8]
τ(C1–O1–C5–C4)	68.64 (67.48)	66.48 (65.72)	61.94 (62.69)	63.21 (62.94)	62.27 (63.76)	63.64
τ(C4–C5–C6–O7)	−166.68 (−164.80)	71.46 (70.63)	−172.43 (−171.48)	−172.18 (−174.33)	−166.04 (−171.97)	68.08
τ(O1–C5–C6–O7)	73.77 (76.12)	−49.3 (−49.96)	67.64 (69.19)	67.81 (66.52)	73.74 (69.12)	−55.31
τ(N15–C1–C2–C3)	133.77 (132.49)	−122.09 (−122.86)	−118.16 (−119.72)	−118.16 (−118.12)	−119.68 (−120.45)	−112.64
τ(N15–C1–O1–C5)	−170.84 (−168.68)	83.70 (84.78)	81.93 (82.98)	81.56 (81.49)	83.38 (83.14)	77.49
τ(C2–C1–N15–S16)	176.85 (175.44)	−173.01 (−172.57)	−172.41 (−170.63)	−172.41 (−175.75)	−169.09 (−166.21)	−166.67
τ(O1–C1–N15–S16)	−61.4 (−62.85)	60.88 (61.20)	61.38 (63.10)	61.46 (58.14)	64.39 (67.50)	67.61
τ(O1–C1–C2–C3)	12.88 (12.33)	4.92 (3.58)	9.13 (7.15)	9.20 (8.83)	7.73 (6.41)	13.46
τ(C1–C2–C3–C4)	1.72 (1.40)	3.82 (4.21)	1.48 (2.59)	1.73 (1.90)	2.29 (2.98)	2.95
Δ*G*	0.00 (1.52)	0.88 (4.27)	0.97 (1.84)	1.07 (0.74)	1.73 (0.00)	
%	60.98 (5.45)	13.74 (0.05)	11.94 (3.18)	10.05 (20.46)	3.29 (70.85)	

Comparison with experimental data is also provided. Gibbs free energies relative to the most stable conformer, in kcal mol^{-1}, and percent contribution of every conformation are also shown. The effect of acetonitrile as solvent on the geometry and the energy is shown in parenthesis.

endo-anomeric effect is not present, and then, a dominant $n_{N15} \rightarrow \sigma^*_{C1-O1}$ leads to a shorter C1–N15 bond. As can be seen from Table 1, the values of the torsion angle C2–C1–N15–S16 show an antiperiplanar relationship between N15H and the H atom bound to C1 in conformers **1** and **3**, in agreement with the $n_{N15} \rightarrow \sigma^*_{C1-O1}$ orbital interaction associated with the *exo*-anomeric effect. The NBO analysis presented in Table 2 shows that the $n_{N15} \rightarrow \sigma^*_{C1-O1}$ orbital interaction is similar for both conformers, whereas the $n_{O1} \rightarrow \sigma^*_{C1-N15}$ orbital interaction is much lower in conformer **3a** than in conformers **1**, thus supporting the experimental findings. It is also interesting to note that solvent effects do not modify the above argument.

Spin–spin coupling constant data for the α anomer[6] indicate a value of 9.8 Hz for $J_{N15H-C1H}$, which is consistent with the presence of an antiperiplanar relationship between N15H and H atom bound to C1. Thus, conformations predicted about the C1–N15 bond in conformers **1** are in very good agreement with the experimental data both in solution and in solid state.

The root mean square deviation, RMSD, for the gas-phase conformers **1** with respect to the structure obtained by X-ray diffraction measurements[8] is calculated with the aid of the Qmol software.[32] Values of 0.26, 0.22, 0.16, and 0.44 Å for the RMSD are obtained for conformers **1a**–**1d**, respectively. It can be seen in Figure 3 that the acetoxymethyl group presents the largest deviation from the solid state geometry in all cases. An appreciable departure from the solid state structure is also observed for the acetoxy group in conformer **1d**. Conformer **1c** exhibits the lowest RMSD with respect to the structure found in the crystal lattice, in clear contrast with the dihedral angle analysis made from Table 1, which suggests that conformer **1a** could present a geometry that resembles more the solid state structure.

Conformational behavior about the C5–C6 bond in carbohydrates leads to three staggered orientations, namely *gauche–gauche* (gg), *trans–gauche* (tg), and *gauche–trans* (gt). All these conformations correspond to local minima on the molecular potential energy surface of the corresponding carbohydrate. Conformers **1b**–**1d** show preference for conformation gt while conformation gg is preferred for conformer **1a** and the solid state structure, see dihedral angle τ(C4–C5–C6–O7) in Table 1. The main difference in the conformation about the C5–C6 bond exhibited by conformer **1c** and the solid state structure of SAE could be explained in terms of a six-membered ring formed by two SAE units. The two hydrogen atoms from the NH_2 group of the sulfamide moiety in a SAE unit and the two oxygen atoms of the sulfamide group of a neighbor SAE unit interact to form a six-membered ring, giving rise to an extended structure in the crystal lattice. The gg orientation of the acetoxymethyl group is then necessary to avoid steric interactions, which will disturb the sulfamide-extended arrangement otherwise.

An interesting finding of the present results is the rather large difference in the C1–C2 bond length between conformer **1c** (1.506 Å) and the solid state structure of SAE (1.477 Å). Examination of the O1–C1–C2–C3 dihedral angle, see Table 1, shows a more distorted ring in the crystal lattice, which in principle could allow a better $\pi_{C2-C3} \rightarrow \sigma^*_{C1-N15}$ orbital interaction. This favorable orbital interaction leads to a shorter C1–C2 bond in the solid state structure of SAE with respect to that in conformer **1c**. Interestingly, this fact is confirmed by the NBO analysis, see Table 2.

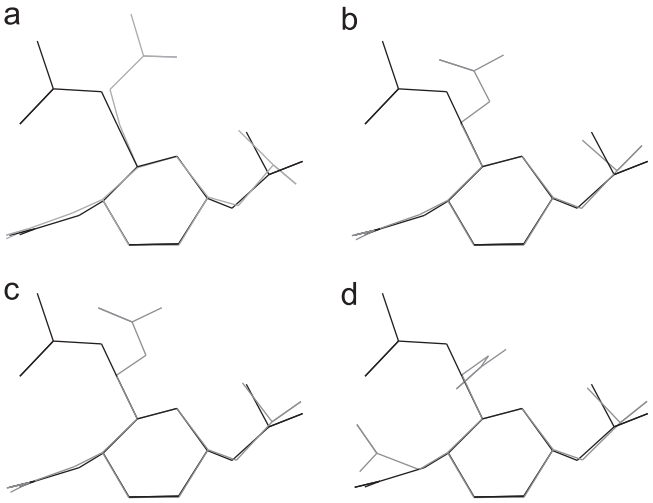

Figure 3. Superimposition of the four conformations **1** obtained in the gas phase with the solid state structure.

Table 3 shows some characteristic geometrical parameters and topological properties of intramolecular hydrogen bonds found in the five stable conformers of SAE, both in the gas phase and in acetonitrile. The values of the electronic density, ρ, and its laplacian, $\nabla^2\rho$, at the bond critical points indicate that these are hydrogen bonds.[33] Moreover, ellipticity values, ϵ, suggest that the bonds are stable and will not undergo any appreciable distortion to further stabilize the system. It is worth noting that there is no relationship between the number of intramolecular hydrogen bonds formed by the different conformers and their relative stability measured as Gibbs free energy differences. This is valid both for gas-phase and C-PCM calculations. The most stable conformer in the gas phase, **3a**, is the only species forming a hydrogen bond between the hydrogen atom bound to C10 in the acetoxymethyl group and O17 in the sulfamide group. On the other hand, both conformers **3a** and **1a** present a hydrogen bond formed by O9 in the acetoxymethyl group and a hydrogen atom attached to N18 in the sulfamide group. It is then argued that these hydrogen bonds should contribute to the relative stability of the different conformations found for SAE in the gas phase. When solvent effects are included through C-PCM the intramolecular hydrogen bonds of the O···HC form become removed, clearly suggesting that these could be formed in the gas phase only. The hydrogen bonds formed by different oxygen atoms and a hydrogen atom attached to N18 in the sulfamide group remain after the incorporation of solvent

Table 2
Natural bond orbital interaction energies, in kcal mol^{-1}, of the different conformers calculated for SAE in the gas phase

Orbital interaction	3a	1a	1b	1c	1d	Experimental
$n_{O1} \rightarrow \sigma^*_{C1-N15}$	2.72 (2.81)	11.63 (11.95)	12.47 (12.45)	11.84 (12.33)	12. 44 (12.17)	12.14
$n_{N15} \rightarrow \sigma^*_{C1-O1}$	13.47 (12.7)	14.26 (13.17)	14.62 (13.95)	15.13 (13.65)	14. 49 (13.95)	14.69
$\pi_{C2-C3} \rightarrow \sigma^*_{C1-N15}$ [a]	3.82	4.89	4.87	4.86	4.89	5.95

The column labeled *Experimental* shows the NBO analysis carried out on the frozen solid state geometry[8] at the B3LYP/6-31++G(d,p) level of theory. The effect of acetonitrile as solvent is shown in parenthesis, except for the last NBO interaction.

[a] π_{C2-C3} is indeed the second σ_{C2-C3} bond orbital, which is supposed to describe the double bond between C2 and C3.

Table 3
Bond lengths (r, in Å), bond angles (α, in degrees) and selected topological properties (see text for the meaning of the symbols) of intramolecular hydrogen bonds of the five stable conformers of 4,6-di-*O*-acetyl-2,3-dideoxy-D-*erythro*-hex-2-enopyranosyl sulfamide found in the present work

Conformer	Bond	r(X···H)	r(X···Y)	α(X···HY)	$\rho \times 10^2$	$\nabla^2\rho \times 10^2$	$\epsilon \times 10^1$
3a	O13···HC6	2.79	3.42	116.55	0.58	2.22	1.42
	O17···HC10	3.35	4.17	131.99	0.14	0.60	3.04
	O9···HN18	2.06	3.07	170.97	1.82	5.67	0.71
	O1···HN18	2.47	3.04	114.3	0.96	3.84	2.39
	O9···HN18	2.13	3.10	158.7	1.59	5.01	0.71
1a	O9···HN18	2.19	3.18	161.44	0.14	4.39	0.59
	O1···HN18	2.47	3.02	113.0	1.08	4.09	4.02
	O9···HN18	2.22	3.21	161.3	1.32	4.15	0.44
1b	O1···HN18	2.54	3.13	116.28	0.89	3.44	3.18
	O7···HN18	2.45	3.29	138.24	0.87	3.20	1.43
	O1···HN18	2.53	3.16	119.3	0.90	3.39	2.63
	O7···HN18	2.52	3.34	136.6	0.75	2.90	1.46
1c	O1···HN18	2.43	3.14	126.02	1.12	3.84	2.67
	O7···HN18	2.41	3.25	138.86	0.98	3.46	0.92
	O1···HN18	2.50	3.19	123.9	0.99	3.49	3.79
	O7···HN18	2.31	3.22	147.6	1.16	3.85	0.73
1d	O13···HC6	2.68	3.41	80.82	0.70	2.64	2.48
	O1···HN18	2.51	3.11	117.03	0.96	3.59	2.63
	O7···HN18	2.66	3.37	126.2	0.61	2.48	2.41
	O7···HN18	2.88	3.49	118.5	0.40	1.72	5.81

The upper set of data for every conformer corresponds to gas-phase results, whereas the lower set corresponds to C-PCM results.

Table 4
Experimental and gas-phase calculated IR vibrational frequencies, in cm^{-1}, of 4,6-di-*O*-acetyl-2,3-dideoxy-D-*erythro*-hex-2-enopyranosyl sulfamide

Experimental	Calculated	Assignment
1024	1013	Stretching ring C–O–C
1160	1091, 1101	Symm strecthing SO_2
1260	1202, 1214	Asymm stretching C–O–C
1355	1300	Asymm stretching SO_2
1426	1422–1429	Asymm bending CH_3
1574	1537	Scissor NH_2
1732	1741	Stretching C=O
2852	2907	Stretching CH
2925	2978	Stretching CH
2965	3018	Stretching CH
3282	3338	Sym stretching NH_2
3338	3436	Stretching NH
3409	3470	Asym stretching NH_2

Calculated frequencies are obtained as a Maxwell–Boltzmann statistically averaged over the four conformers **1**.

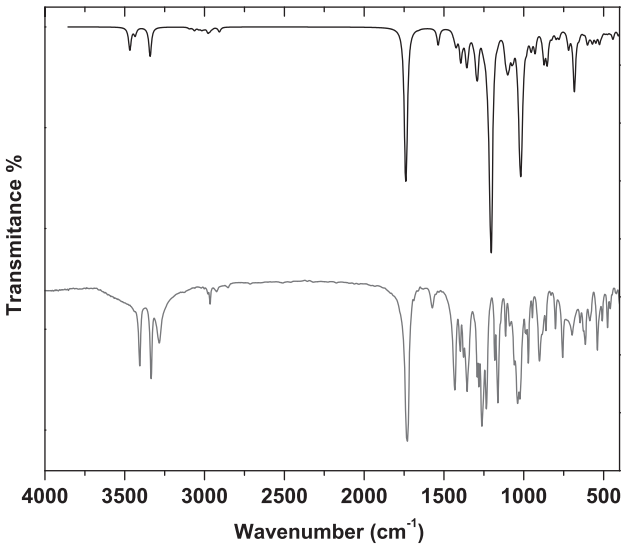

Figure 4. Experimental (grey) and calculated (black) IR spectra of 4,6-di-*O*-acetyl-2,3-dideoxy-D-*erythro*-hex-2-enopyranosyl sulfamide. The calculated spectrum is obtained as a statistical average of the four gas-phase conformers **1** found in the present work.

effects. As expected according to the small changes in the geometry observed in Table 1, no appreciable modifications are seen either in the geometrical or in the topological parameters of the hydrogen bonds.

Table 4 shows some of the more relevant experimental vibrational frequencies of SAE obtained in the present work. It should be pointed out that solid samples, from which the IR spectrum is obtained contains α anomer only. Taking into account that experimental fact, statistically averaged theoretical frequencies of gas-phase conformers **1** are given in Table 4. A proposed assignment is also given. It can be seen from the table that scaled frequencies agree well with the experimental data. It can also be seen from Figure 4, which depicts the experimental and simulated IR spectra, that despite important discrepancies in the relative intensities between experimental and calculated bands, maxima positions are well described by the theoretical methodology used throughout the present work.

The preferred anomeric configuration of α isomer of SAE has been assigned by high-resolution NMR spectroscopy.[8] As sulfonamidoglycosylation afforded almost exclusively the α anomer, NMR studies of the β anomer could not be performed. It is shown in Table 5 and Figure 5 the comparison of experimental and calculated ^1H and ^{13}C chemical shifts for α anomer, respectively. Chemical shifts calculated in the gas phase are presented as a Maxwell–Boltzmann statistical-averaged of the four conformers **1**. In these cases in which a single signal due to several equivalent atoms is experimentally observed, the corresponding calculated chemical shifts of the involved atoms are averaged. It can be seen from the table that the agreement with experimental data is quite good in general. The largest error in ^1H chemical shifts is observed for NH and NH_2 of the sulfamide group and could be attributed to intermolecular hydrogen bonds formed in acetonitrile solution. These intermolecular hydrogen bonds could not be mimiced by an implicit method like C-PCM.

Sulfonamidoglycosylation of 3,4,6-tri-*O*-acetyl-D-glucal with sulfamide afforded SAE in an α/β ratio of 95:5.[6] As stated above,

Table 5
Experimental and gas-phase calculated ^{1}H and ^{13}C chemical shifts, in ppm, of 4,6-di-*O*-acetyl-2,3-dideoxy-D-*erythro*-hex-2-enopyranosyl sulfamide

Atom	Experimental[8]	Calculated
H1	5.45	5.78
H2	5.86	6.12
H3	5.97	6.30
H4	5.23	5.45
H5	4.02	3.99
H6a	4.07	3.79
H6b	4.29	4.87
H10a,b,c	2.02	2.04
H14a,b,c	2.08	2.10
H15	6.43	4.68
H18a,b	5.35	4.80
RMSD		0.61
C1	78.4	83.43
C2	127.7	134.83
C3	130.4	139.70
C4	65.5	70.38
C5	67.9	71.58
C6	64.1	67.02
C8	171.3	179.52
C10	20.9	21.23
C12	171.1	178.54
C14	21.2	21.66
RMSD		5.98

Calculated chemical shifts are obtained as a Maxwell–Boltzmann statistical-averaged over the four conformers **1**. See Figure 1 for labels.

the present results show the same ratio when solvent effects (acetonitrile) are considered implicitly, which seems to indicate that the synthesis of the sulfamide under study should occur mainly under thermodynamic control. It is a well-known fact that N-glycosylation of carbohydrates afforded β-isomers as major products.[34] That fact could be explained in terms of interactions present in the axial isomer of glucopyranosylamines mainly due to the conformation of the anomeric nitrogen, thereby favoring the equatorial isomer, in which that interaction is absent.[35] It was stated above that a $n_{N15} \rightarrow \sigma^{*}_{C1-O1}$ orbital interaction favors an antiperiplanar relationship between N15H and the hydrogen atom bound to C1. In α-glucosylpyranoses that conformation necessarily locates the hydrogen atom attached to C1 under the pyranose ring, giving an enhanced steric effect.[5] In the present 2,3-enopyranosyl α-isomer, on the other hand, the situation is different. Examination of dihedral angles indicates an almost planar conformation of C1–C2–C3–C4, thus the unfavorable steric interaction described is absent. In summary, the stereochemical outcome of sulfonamidoglycosylation with sulfamide could be tentatively explained as a combination of several factors including the absence of steric interactions due to the conformation of the anomeric nitrogen in the α-isomer, which enables the *exo*-anomeric interaction and a $n_{O1} \rightarrow \sigma^{*}_{C1-N15}$ orbital interaction (*endo*-anomeric effect) that it is only present in the α-isomer.

4. Conclusions

The novel 4,6-di-*O*-acetyl-2,3-dideoxy-D-*erythro*-hex-2-enopyranosyl sulfamide has been investigated from a combined theoretical and spectroscopic point of view.

The conformational study of the compound showed that the α anomer becomes thermodynamically more stable than the β one when solvent effects are included in the calculations, leading to an α/β ratio of about 95:5. As experimental methods afford more than 95% of the α form, it is concluded that reaction could very probably proceed with a thermodynamical control.

A detailed analysis of geometrical parameters shed light into the nature of the solid state structure of the novel 4,6-di-*O*-acetyl-2,3-dideoxy-D-*erythro*-hex-2-enopyranosyl sulfamide in terms of *exo*- and *endo*-anomeric effects and antiperiplanar relationships. NBO calculations confirmed those findings. Moreover, optimized geometries agreed quite well with the crystallographic data, the most important discrepancies being observed in the orientation of the acetoxymethyl group.

Several intramolecular hydrogen bonds were found in the stable conformers of the sulfamide under study, in both gas-phase and solvent-including calculations. No relationship seems to exist between the relative stability of the conformers and the amount of intramolecular hydrogen bonds formed. Moreover, some weak hydrogen bonds involving an O···HC bond are removed after the inclusion of solvent effects.

The IR spectrum was recorded and reported for the first time for 4,6-di-*O*-acetyl-2,3-dideoxy-α-D-*erythro*-hex-2-enopyranosyl sulfamide. The assignment of some of the most important bands was accomplished with the aid of calculated vibrational frequencies.

Finally, theoretical calculations of ^{1}H and ^{13}C chemical shifts contribute to a better understanding of the experimental spectra. Present results support previous findings concerning configuration and conformation assignments for 4,6-di-*O*-acetyl-2,3-dideoxy-α-D-*erythro*-hex-2-enopyranosyl sulfamide. Furthermore, present results suggest that the NH group could be involved in intermolecular hydrogen bonds as experimental and gas-phase theoretical chemical shifts exhibit appreciable discrepancies.

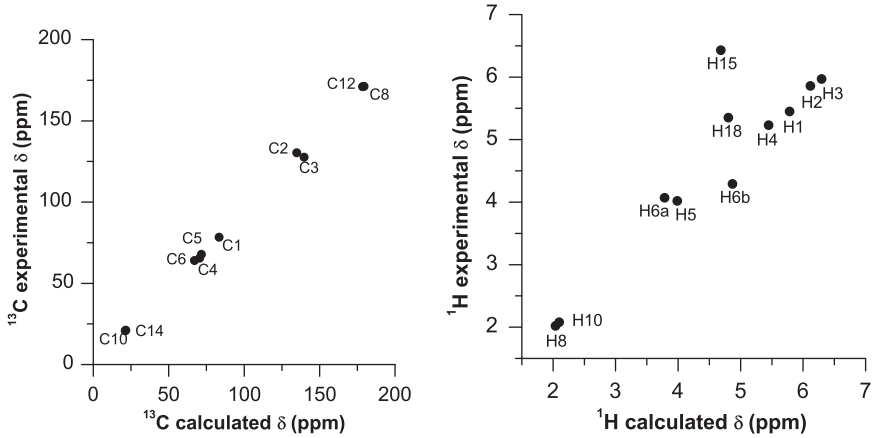

Figure 5. Comparison of calculated and experimental results of ^{13}C and ^{1}H NMR for α anomer of SAE. Calculated data correspond to gas phase results.

In summary, the present methodology appears to be a powerful technique for the study of the conformational space and geometric, vibrational, and magnetic properties of *N*-glycosyl sulfamides.

Acknowledgments

The authors thank CONICET and UNLP for the financial support. P.A.C. and R.P.D. are members of the Scientific Research Career of CONICET. M.J.L. is a fellow of CONICET. The authors gratefully acknowledge Professor Ana C. González Baró, CEQUINOR, UNLP, for her valuable help during IR spectrum recording.

References

1. Krishnamurthy, V. M.; Kaufman, G. K.; Urbach, A. R.; Gitlin, I.; Gudiksen, K. L.; Weibel, D. B.; Whitesides, G. M. *Chem. Rev.* **2008**, *108*, 946–1051.
2. Supuran, C. T. *Nat. Rev. Drug Disc.* **2008**, *7*, 168–181.
3. Thiry, A.; Dognè, J.-M.; Masereel, B.; Supuran, C. T. *Trends Pharmacol. Sci.* **2006**, *27*, 566–573.
4. Winum, J.-Y.; Poulsen, S.-A.; Supuran, C. T. *Med. Res. Rev.* **2009**, *29*, 419–435.
5. Colinas, P. A.; Témpera, C. A.; Rodríguez, O. M.; Bravo, R. D. *Synthesis* **2009**, *24*, 4143–4148. and references cited therein.
6. Colinas, P. A.; Bravo, R. D. *Carbohydr. Res.* **2007**, *342*, 2297–2302.
7. Colinas, P. A.; Bravo, R. D.; Vullo, D.; Scozzafava, A.; Supuran, C. T. *Bioorg. Med. Chem. Lett.* **2007**, *17*, 5086–5090.
8. Colinas, P. A.; Bravo, R. D.; Echeverría, G. A. *Carbohydr. Res.* **2008**, *343*, 3005–3008.
9. Alegre, M. L.; Pis Diez, R.; Colinas, P. A. *J. Mol. Struct.* **2009**, *919*, 223–226.
10. JCBN *Eur. J. Biochem.* **1980**, *111*, 295–298.
11. U. Hypercube Inc., Hyperchem 5.0 for Windows [computer software], **1996**.
12. Dewar, M. J. S.; Zoebisch, E. G.; Healy, E. F.; Stewart, J. J. P. *J. Am. Chem. Soc.* **1985**, *107*, 3902–3909.
13. Berendsen, H. J. C.; Postma, J. P. M.; Van Gunsteren, W.; Dinola, A.; Haak, J. *J. Chem. Phys.* **1984**, *81*, 3684–3690.
14. Hohenberg, P.; Kohn, W. *Phys. Rev.* **1964**, *136*, B864–B871.
15. Kohn, W.; Sham, L. J. *Phys. Rev.* **1965**, *140*, A1133–A1138.
16. Parr, R.; Yang, W. Density Functional Theory of Atoms and Molecules; Oxford University Press, 1989.
17. Frisch, M. J.; Trucks, G. W.; Schlegel, H. B.; Scuseria, G. E.; Robb, M. A.; Cheeseman, J. R.; Montgomery, J. A., Jr.; Vreven, T.; Kudin, K. N.; Burant, J. C.; Millam, J. M.; Iyengar, S. S.; Tomasi, J.; Barone, V.; Mennucci, B.; Cossi, M.; Scalmani, G.; Rega, N.; Petersson, G. A.; Nakatsuji, H.; Hada, M.; Ehara, M.; Toyota, K.; Fukuda, R.; Hasegawa, J.; Ishida, M.; Nakajima, T.; Honda, Y.; Kitao, O.; Nakai, H.; Klene, M.; Li, X.; Knox, J. E.; Hratchian, H. P.; Cross, J. B.; Bakken, V.; Adamo, C.; Jaramillo, J.; Gomperts, R.; Stratmann, R. E.; Yazyev, O.; Austin, A. J.; Cammi, R.; Pomelli, C.; Ochterski, J. W.; Ayala, P. Y.; Morokuma, K.; Voth, G. A.; Salvador, P.; Dannenberg, J. J.; Zakrzewski, V. G.; Dapprich, S.; Daniels, A. D.; Strain, M. C.; Farkas, O.; Malick, D. K.; Rabuck, A. D.; Raghavachari, K.; Foresman, J. B.; Ortiz, J. V.; Cui, Q.; Baboul, A. G.; Clifford, S.; Cioslowski, J.; Stefanov, B. B.; Liu, G.; Liashenko, A.; Piskorz, P.; Komaromi, I.; Martin, R. L.; Fox, D. J.; Keith, T.; Al-Laham, M. A.; Peng, C. Y.; Nanayakkara, A.; Challacombe, M.; Gill, P. M. W.; Johnson, B.; Chen, W.; Wong, M. W.; Gonzalez, C.; Pople, J. A. GAUSSIAN *03, revision d.01* [computer software], 2004.
18. Becke, A. *J. Chem. Phys.* **1993**, *98*, 5648–5652.
19. Lee, C.; Yang, W.; Parr, R. G. *Phys. Rev. B* **1988**, *37*, 785–789.
20. Stephens, P.; Devlin, F.; Chabalowski, C.; Frisch, M. *J. Phys. Chem.* **1994**, *98*, 11623–11627.
21. National Institute of Standards and Technology, Computational chemistry comparison and benchmark database, http://cccbdb.nist.gov/.
22. Cheeseman, J. R.; Trucks, G. W.; Keith, T. A.; Frisch, M. J. *J. Chem. Phys.* **1996**, *104*, 5497–5509.
23. Ditchfield, R. *Mol. Phys.* **1974**, *27*, 789–807.
24. Wolinski, K.; Hinton, J. F.; Pulay, P. *J. Am. Chem. Soc.* **1990**, *112*, 8251–8260.
25. Reed, A. E.; Curtiss, L. A.; Weinhold, F. *Chem. Rev.* **1988**, *88*, 899–926.
26. Bader, R.. *Atoms in Molecules. A Quantum Theory*. In *International Series of Monographs on Chemistry*; Clarendon Press: Oxford, 1990.
27. Keith, T. A. Aimall version 09.02.01 [computer software], aim.tkgristmill.com, 2009.
28. Barone, V.; Cossi, M. *J. Phys. Chem. A* **1998**, *102*, 1995–2001.
29. Cossi, M.; Rega, N.; Scalmani, G.; Barone, V. *J. Comput. Chem.* **2003**, *24*, 669–681.
30. Lichtenthaler, F. W.; Werner, B. *Carbohydr. Res.* **1999**, *319*, 47–54.
31. Pinto, B.; Schlegel, H.; Wolfe, S. *Can. J. Chem.* **1987**, *65*, 1658–1662.
32. Gans, J.; Shalloway, D. Qmol [computer software], *J. Mol. Graphics Modell.* **2001**, *19*, 557–559.
33. Koch, U.; Popelier, P. L. A. *J. Phys. Chem.* **1995**, *99*, 9747–9754.
34. Norris, P. *Curr. Top. Med. Chem.* **2008**, *8*, 101–113.
35. Batchelor, R.; Green, D.; Johnston, B.; Patrick, B.; Pinto, B. *Carbohydr. Res.* **2001**, *330*, 421–426.